

# COMPARISON OF THE INERTIAL RESPONSE OF THE THOR-NT, HYBRID III, AND UNEMBALMED CADAVER TO SIMULATED KNEE-TO-KNEE-BOLSTER IMPACTS

**Jonathan D. Rupp, Matthew P. Reed,**

**Nathaniel H. Madura, Carl S. Miller**

University of Michigan Transportation Research  
Institute, USA

**Shashi Kuppa**

National Highway Traffic Safety Administration,  
USA

**Lawrence W. Schneider**

University of Michigan Transportation Research  
Institute, USA

Paper Number 05-0086

## ABSTRACT

The inertial responses of five seated unembalmed midsize cadavers to sub-injury knee impact loading were characterized and compared to the inertial responses of the Hybrid III midsize male and THOR-NT ATDs collected under similar knee loading conditions. All impacts were performed using a 275-kg padded impactor to symmetrically load the left and right knees at velocities of either 1.2 or 3.5 m/s. At both knee impact velocities, the Hybrid III and THOR-NT produced peak knee impact forces that were substantially higher than those of the cadaver. At the 1.2 m/s impact velocity, the peak knee impact forces produced by the cadavers varied from 0.9 to 1.0 kN while the peak knee impact forces produced by the THOR and Hybrid III were 1.4 and 1.6 kN, respectively. The two cadavers tested at the 3.5 m/s impact velocity produced peak applied forces of 3.5 and 3.8 kN, while the THOR and Hybrid III produced peak applied forces averaging 5.5 and 6.1 kN, respectively.

For both knee impact velocities, femur and pelvis accelerations produced by both ATDs and the cadavers were similar in magnitude. However, peaks in cadaver femur and pelvis accelerations occurred substantially earlier than peaks in cadaver knee impact force, while peak Hybrid III and THOR femur and pelvis accelerations occurred at the time of peak force. These differences are most likely due to loosely coupled mass in the cadaver that is not represented in either ATD.

## INTRODUCTION

Fractures and dislocations of the knee-thigh-hip (KTH) complex in frontal crashes are of substantial concern to automotive safety engineers and clinicians because of the frequency at which these injuries occur and the associated potential for long-term disability (Kuppa et al. 2001, Read et al. 2002, Burgess et al. 1999). Of all AIS 2+ KTH injuries, hip injuries, and in particular acetabular fractures, are the most frequent, occurring at a rate of almost 14,000 per year (Rupp et al. 2001).

A research program is underway at the University of Michigan Transportation Research Institute to develop new KTH injury criteria that can assess the risk of hip injury in frontal crashes. To date, this program has demonstrated that under dynamic knee loading, the hip has a tolerance of 6.1 kN and is the weakest component of the KTH complex with the pelvis and femurs oriented in a seated automotive posture (Rupp et al. 2002, 2003a). The 6.1-kN hip tolerance was determined using a fixed pelvis boundary condition and is therefore representative of the fracture tolerance of the hip in terms of force applied to the hip. However, under real-world knee-to-knee-bolster loading, the force at the knee is greater than the force at the hip because there is mass proximal and distal to the hip that is decelerated by knee-bolster impact. To determine the risk of hip injury associated with a force applied to the knee, it is therefore necessary to know the decrease in force between the knee and the hip, which is governed by the inertial response of the knee-thigh-hip complex. In addition, to develop improved KTH injury criteria it is necessary to know how forces measured by ATD load cells relate to force at the human hip under similar knee impact conditions.

Horsch and Patrick (1976) attempted to characterize the inertial response of the cadaver to knee impact loading by measuring force applied to the knees of unembalmed cadavers and the resulting femur accelerations under high-rate sub-fracture impact loading by a flat-faced rigid ballistic pendulum. Inertial response of the cadaver to knee impact loading was reported as an effective mass, which was calculated by dividing the force applied to the knee by the acceleration of the femur. For the four cadavers tested, the effective mass of each side of the

body was approximately 2.0 kg immediately prior to the time of peak force, after which femur acceleration rapidly approaches zero and the effective mass calculation fails.

Because Horsch and Patrick used a rigid impactor, peak forces occurred approximately 2 ms after the onset of knee loading. Stalnaker et al. (1977) have shown that it takes 2-5 ms after the start of force application for a reaction force to be developed at the pelvis. In other words, 2-5 ms are needed for the femur to displace a sufficient amount to start recruiting the mass of the pelvis. Thus, the 2.0 kg effective mass value reported by Horsch and Patrick is likely representative of the effective mass of the skeletal knee/femur complex and does not accurately represent effective mass of one side of the body under longer-duration knee impacts, such as those observed in FMVSS 208 and NCAP.

Horsch and Patrick also characterized the inertial response of the Hybrid II ATD in the same manner that cadaver inertial response was characterized. The effective mass of the Hybrid II under impact of one knee was approximately 11.5 kg. The Hybrid II also produced peak knee impact forces that were 1.5 to 3.7 times greater than those produced in the cadaver knee impacts. The hypothesized reasons for the differences between Hybrid II and cadaver response were that the Hybrid II KTH complex is stiffer and has more tightly coupled mass than the cadaver.

The current study expands on the data collected by Horsch and Patrick by characterizing the inertial response of unembalmed cadavers under longer duration knee loading conditions and comparing these inertial responses to those of the Hybrid III and THOR-NT ATDs.

## METHODS

### Cadaver Tests<sup>1</sup>

The characteristics of the five unembalmed cadavers used in this study are listed in Table 1. All subjects were males that were close to the 176 cm midsize male stature. Subject masses varied from 66 to 89 kg and averaged 77 kg.

Figure 1 shows the apparatus used to determine the inertial response of the cadavers under knee impact loading. Simultaneous loads are applied to the left and right knees of a seated cadaver by pneumatically accelerating a 275-kg platform to a velocity of 1.2 m/s or 3.5 m/s prior to knee impact. Load cells on the forward surface of the platform were used to independently measure the force applied to the left and right cadaver knees. The acceleration of the mass on the forward surface of each load cell was measured and used to inertially compensate all force measurements. As shown on the right-hand side of Figure 1, the left and right knee impact surfaces were padded. For the 1.2 m/s knee impacts, each knee was padded with 38-mm thick 50-durometer (Shore OO scale) Sorbethane padding. As indicated in Table 1, this combination of padding and impact velocity was used in tests of all five cadavers.

Because the 1.2 m/s knee impact condition produced peak forces and loading rates that were substantially less than those produced in FMVSS 208 and NCAP compliance tests, a second set of impacts was performed to determine how the inertial response of the cadaver changes when the knee is loaded with forces and loading rates that are more representative of those produced in FMVSS 208 and NCAP tests. The higher loading rates and higher knee impact forces in this second test condition were generated by increasing impactor velocity to 3.5 m/s and padding the knee impact surface with 25 mm 70-durometer Sorbethane and 25-mm thick 50-durometer Sorbethane.

Cadavers were instrumented by rigidly attaching triaxial accelerometer blocks to the midshaft femur and sacrum. Each cadaver was dressed in a Lycra leotard. Prior to each test, the cadaver was seated on a force platform that was covered with a low friction surface to ensure that friction on the pelvis and thighs did not substantially affect the force applied to the knee. Shear forces measured by the force platform were used to verify that friction forces were low in all tests (< 50 N in the 1.2 m/s tests and less than < 150 N for the 3.5 m/s tests). The fore-aft position of the cadaver on the force platform was adjusted to ensure that the cadaver was able to slide 15-20 cm rearward on the platform prior to contact between the posterior leg and the forward surface of the force platform.

---

<sup>1</sup> The rights, welfare, and informed consent of the subjects who participated in this study were observed under guidelines established by the U.S. Department of Health and Human Services on Protection of Human Subjects and accomplished under medical research design protocol standards approved by the Committee to Review Grants for Clinical Research and Investigation Involving Human Beings, Medical School, The University of Michigan.

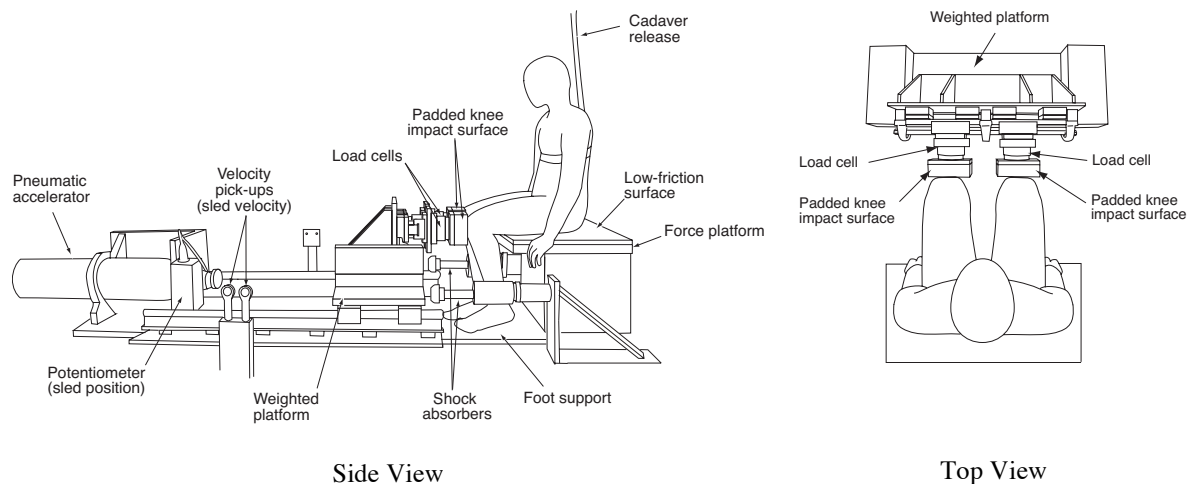


**Figure 1. Apparatus used for dynamic femur response assessment.**

The cadaver's feet were supported by a second force platform. The heights of the foot support and the cadaver-seating platform were adjusted so that the long axis of the femur was horizontal. The fore-aft positions of the cadaver's feet were adjusted so that the included angle between the tibia and the femur was approximately 90°. The lateral spacing between the centers of the knee impact surfaces was adjusted so that, in an overhead view, the shaft of the femur was aligned with the direction of impact.

**Table 1. Cadaver Characteristics and Test Conditions**

Subject Number	Gender	Age	Stature (cm)	Mass (kg)	Knee Impact Velocity	
					1.2 m/s	3.5 m/s
1	M	66	179	89	X	
2	M	64	178	82	X	
3	M	66	178	73	X	
4	M	76	178	70	X	X
5	M	82	180	66	X	X
	<i>Mean</i>	70.8	178.6	76.0		
	<i>sd</i>	7.8	0.9	9.4		

The cadaver's torso was held in an upright position by a strap that was looped under the cadaver's arms and around the cadaver's chest and connected to a release mechanism. About 20 ms prior to knee impact, the release mechanism was actuated, thereby allowing the cadaver to move rearward with minimal constraint during impact loading.

Because any asymmetry in cadaver knee positions could result in differences in the magnitudes and the phasing of the forces applied to the knees, a repetitive test protocol was used. The knees of each cadaver were impacted multiple times until three to five impacts had been performed on each cadaver for

which the magnitudes and phasing of the applied forces were very close. Overhead and side view high-speed videos of the impact event were recorded and used to ensure that the cadaver knees were symmetrically contacted, that the cadaver was released prior to impact, and that the kinematics of the left and right sides of the body were similar.

As shown in the Appendix, forces applied to the left and right knees and the left and right resultant femur accelerations from each test on the same subject were similar and were therefore averaged at each point in time to determine an average resultant femur acceleration and average applied force. The average applied forces, average femur accelerations, and pelvis accelerations in repeated tests on the same subject were also similar and were averaged to determine a representative applied force and femur and pelvis accelerations for each subject.

For each test performed on a subject, the inertial resistance to motion of the left and right sides of the body were calculated as described by Equation 1, where the forces applied to the left and right knees are divided by the resultant pelvis acceleration to determine effective masses. Left- and right-sided effective mass histories calculated using pelvis acceleration were similar and were therefore averaged to determine a single pelvis-acceleration-based effective-mass response for each test.

Effective mass histories from each subject were also calculated, as described in Equation 2, by dividing the left and right applied force by the left and right resultant femur accelerations, respectively. An average femur-acceleration-based effective-mass history for each test was calculated by averaging the

left and right effective mass histories calculated using femur acceleration.

Each set of femur- and pelvis-acceleration-based effective-mass histories from repeated tests on single subject were similar and were therefore averaged to determine a single femur-acceleration-based effective mass history and a single pelvis-acceleration-based effective-mass history for each subject.

$$M_{eff} = \frac{F_{\text{applied to knee}}}{a_{\text{pelvis resultant}}} \quad [1]$$

$$M_{eff} = \frac{F_{\text{applied to knee}}}{a_{\text{femur resultant}}} \quad [2]$$

To provide a reference point for comparing effective mass histories, the effective mass at the time of peak force was determined from each of the average left and right-sided effective mass curves. The range associated with each peak effective mass value was also determined using the average of the left and right effective mass values from each of the repeated tests on a single subject.

### Hybrid III and THOR-NT Response Tests

The inertial responses of the Hybrid III and THOR-NT were determined using the same test apparatus and test procedures described for the cadaver tests. Repeated tests were performed at impact velocities of 1.2 m/s and 3.5 m/s until five tests had been performed where the timing of the left and right knee contacts was similar. Force applied to the ATD knees and accelerations of the femur and pelvis were measured.

Each ATD was equipped with tri-axial pelvis accelerometer blocks and left and right six-channel femur load cells. The THOR-NT was also equipped with the standard 3-axis acetabular load cells. Tri-axial accelerometer blocks were mounted to the mid shaft of the Hybrid III femur and to the THOR femur proximal to the compliant element. Prior to testing, the knee-thigh-hip response of the THOR and the knee response of the Hybrid III were calibrated using standard procedures (Society of Automotive Engineers 1998, Shams 2004).

ATD positioning for all tests was similar to the cadaver positioning. Both ATDs sit upright with minimal assistance, so the release mechanism was not needed in the ATD tests.

## RESULTS

### Cadaver Responses

#### 1.2 m/s Knee Impacts

Figure 2 compares the applied force histories from each of the five cadavers. Applied force histories from all tests were similar with peak applied forces varying between 900 and 1000 N. Figures 3 and 4 compare the average pelvis and femur acceleration histories. Acceleration at the time of peak force is indicated in Figures 3 and 4 by a filled circle. Both femur and pelvis accelerations peak at between 6 and 8 g. In addition, both femur and pelvis accelerations peak approximately 6-8 ms earlier than the time of peak applied force. Figure 5 illustrates that, until the time of peak acceleration, femur acceleration leads pelvis acceleration.

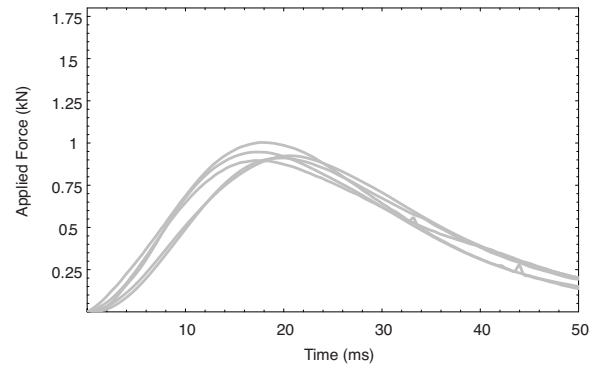


**Figure 2. Applied force histories from cadaver tests at the 1.2 m/s impact velocity.**

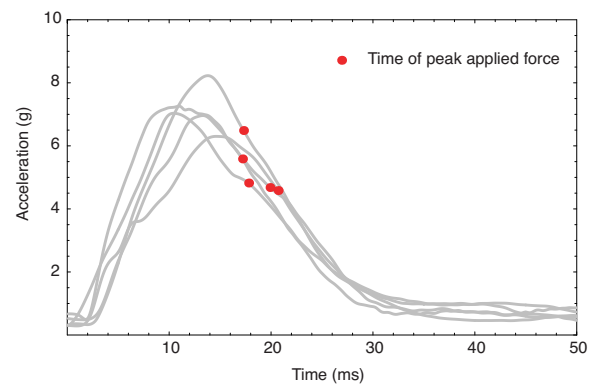


**Figure 3. Resultant pelvis accelerations from cadaver tests at the 1.2 m/s impact velocity.**

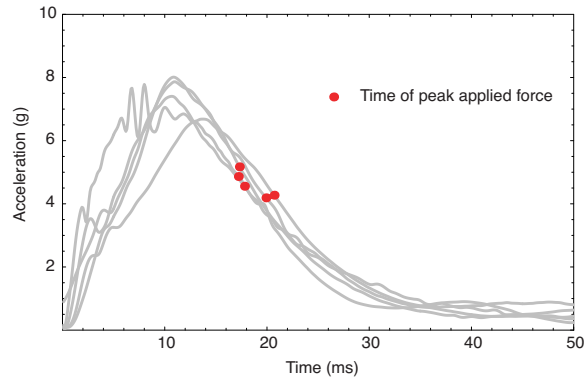


**Figure 4. Resultant pelvis accelerations from cadaver tests at the 1.2 m/s impact velocity.**

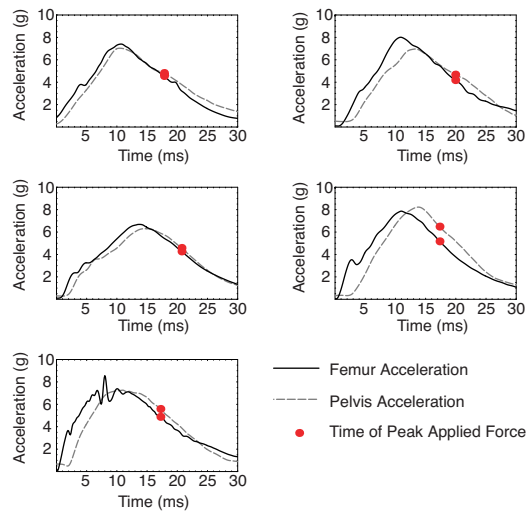


**Figure 5. Femur and pelvis accelerations from all cadaver tests at the 1.2 m/s impact velocity.**

Figures 6 and 7 show the effective mass histories from each cadaver calculated using the resultant pelvis and femur accelerations, respectively. The shaded regions in Figures 6 and 7 are where the effective mass calculation fails because femur and pelvis accelerations are low, and consequently, small variations in acceleration result in large changes in effective mass values. Figures 6 and 7 both show that the effective mass of the cadaver is initially low and then steadily rises over the course of the loading event. The effective mass history calculated using pelvis acceleration is initially higher than the effective mass history calculated using femur acceleration because pelvis acceleration is initially lower than femur acceleration and consequently, when the same applied force is divided by pelvis acceleration, a higher effective mass is produced.

Table 2 lists the effective masses at the time of peak force calculated using femur and pelvis accelerations for each of the five cadavers. The overall average effective mass at the time of peak force calculated using pelvis acceleration is 20.4 kg (Range: 17.2-26.1 kg). The overall average effective mass at the time of peak force calculated using resultant femur acceleration is 21.4 kg (Range: 14.9-23.3).

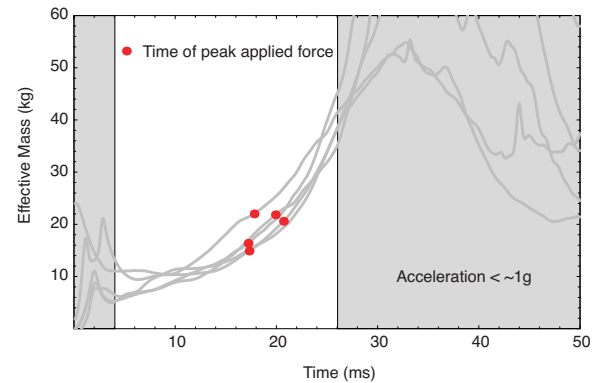


**Figure 6. Pelvis-accleration-based-effective-mass histories from cadaver tests at the 1.2 m/s impact velocity.**

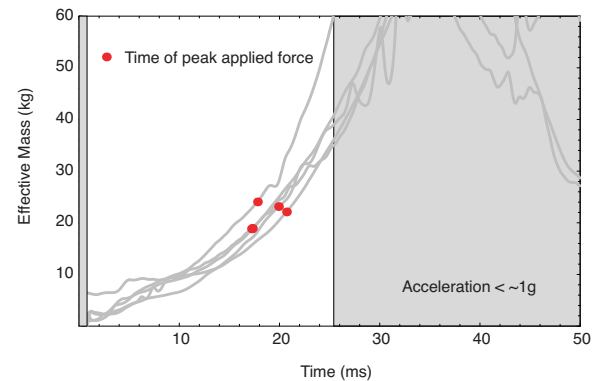


**Figure 7. Femur-accleration-based-effective-mass histories from cadaver tests at the 1.2 m/s impact velocity.**

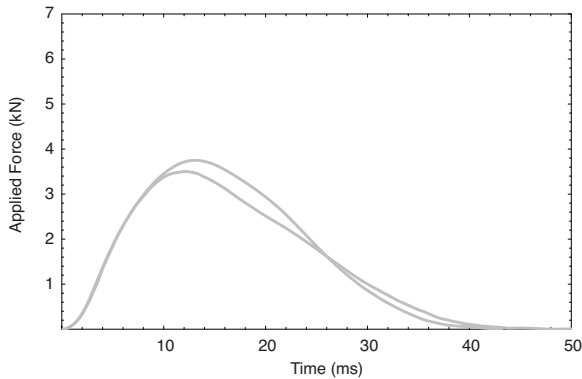
**Table 2. Cadaver Effective Mass at the Time of Peak Applied Force at the 1.2 m/s Impact Velocity**

Subject	Calculated with Pelvis Acceleration, kg (Min-Max)	Calculated with Femur Acceleration, kg (Min-Max)
1	22.0 (21.3-23.3)	24.1 (21.2-26.1)
2	21.8 (19.1-22.7)	23.1 (19.0-23.1)
3	20.6 (20.1-21.0)	22.1 (21.2-22.6)
4	14.9 (14.9-15.5)	18.9 (17.2-20.0)
5	16.4 (16.2-16.6)	18.8 (18.7-19.0)
Overall Average (Range)	20.4 (17.2-26.1)	21.4 (14.9-23.3)

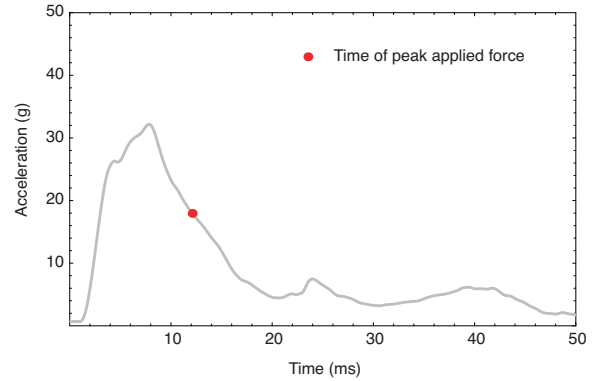
### 3.5 m/s Knee Impacts

Figure 8 shows the force histories from the two sets of sub-injury effective mass tests that were performed at the 3.5 m/s knee impact velocity. Peak forces for these tests are 3.5 and 3.8 kN.

Figure 9 shows the resultant pelvis acceleration from one of the two sets of cadaver tests that were performed at the 3.5 m/s knee impact velocity. Instrumentation problems preventing the collection of pelvis accelerations from the other set of tests at the same impact velocity, and pelvis accelerations from this subject were therefore excluded from Figure 9. Figure 10 shows the average resultant femur accelerations from the two cadavers that were tested at the 3.5 m/s impact velocity. Figures 9 and 10 also illustrate the pelvis and femur accelerations at the time of peak applied force. As was the case at the lower impact velocity, both the cadaver femur and pelvis accelerations peak earlier than applied force peaks.



**Figure 8. Applied force histories from cadaver tests at the 3.5 m/s impact velocity.**



**Figure 9. Resultant pelvis acceleration from the single cadaver test at the 3.5 m/s impact velocity.**

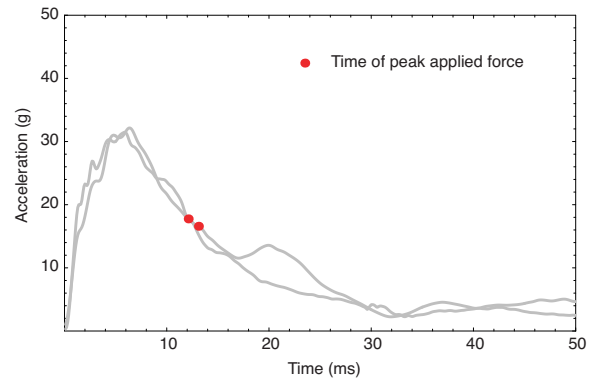


**Figure 10. Resultant femur accelerations from cadaver tests at the 3.5 m/s impact velocity.**

Figures 11 and 12 show the effective mass histories calculated from pelvis and femur accelerations, respectively. Both of these effective mass histories are similar to their lower speed counterparts. That is, Figures 11 and 12 show that cadaver effective mass increases until slightly after the time of peak force. The effective mass history calculated using pelvis acceleration is initially higher than the effective mass history calculated using femur acceleration because pelvis acceleration is initially lower than femur acceleration and consequently, when the same applied force is divided by pelvis acceleration, a higher effective mass is produced.

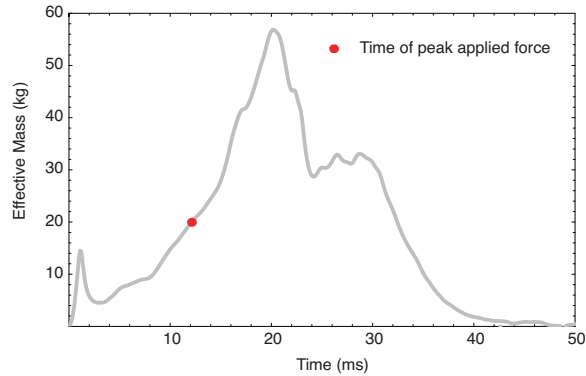


**Figure 11. Pelvis-acceleration-based effective mass history from the 3.5 m/s impact velocity.**

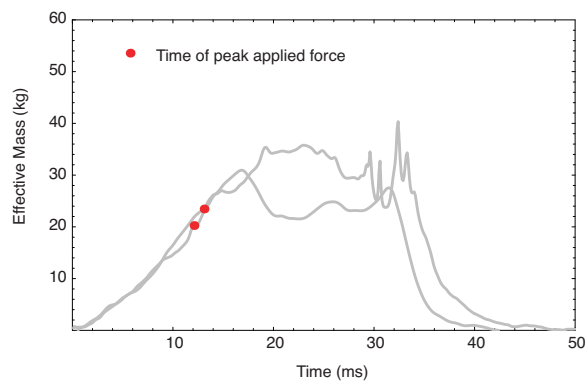


**Figure 12. Femur-acceleration-based effective mass histories from cadaver tests at the 3.5 m/s impact velocity.**

Table 3 lists the effective masses at the time of peak force calculated using femur and pelvis accelerations. The effective mass at the time of peak force calculated using pelvis acceleration is 20.0 kg (Range: 19.2-21.3 kg) for the single subject where pelvis accelerations were successfully measured. The effective masses at the time of peak force calculated using resultant femur acceleration are 23.5 kg (Range: 22.5-24.4 kg) and 20.3 kg (Range: 19.8-22.2 kg). These values and the ranges of these values are greater than the effective mass values and associated ranges from Subjects 4 and 5 calculated from the 1.2 m/s impact data.

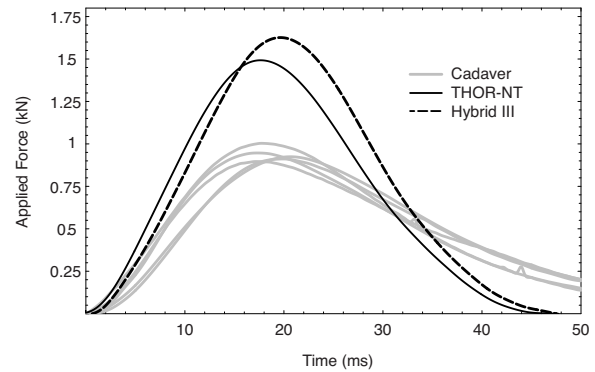
**Table 3. Effective Mass From Cadaver Tests at the Time of Peak Force at the 3.5 m/s Impact Velocity**

Subject	Calculated with Pelvis Acceleration, kg (Min-Max)	Calculated with Femur Acceleration, kg (Min-Max)
4		23.5 (22.5-24.4)
5	20.0 (19.2-21.3)	20.3 (19.8-22.2)

## THOR-NT, Hybrid III and Cadaver Responses

### 1.2 m/s Knee Impacts

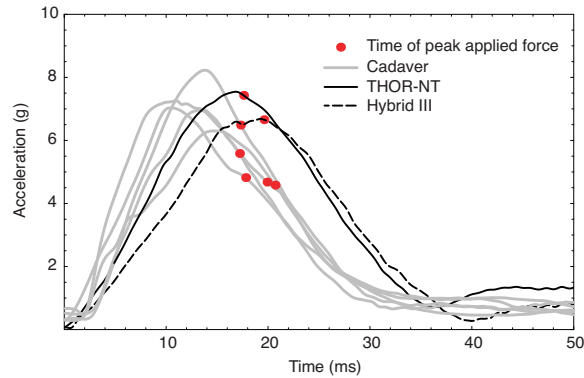
Figure 13 compares the knee impact forces from 1.2 m/s cadaver tests to similar impacts to the knees of the Hybrid III and THOR-NT ATDs. The knee impact forces produced by the THOR-NT averaged to approximately 1.4 kN, while the knee impact forces produced in tests with the Hybrid III averaged to approximately 1.6 kN. These values are both substantially greater than the 940 N average peak knee impact force produced in cadaver tests.



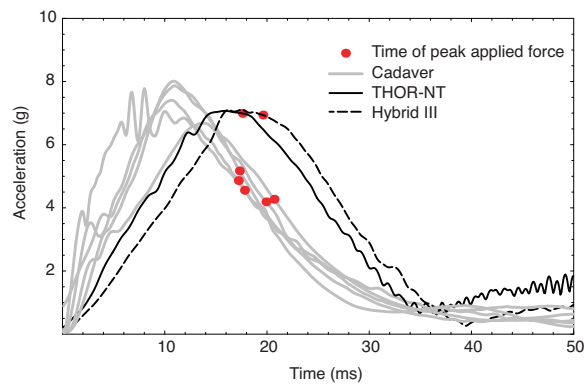
**Figure 13. Comparison of cadaver applied force histories with applied force histories applied to THOR-NT and Hybrid III at the 1.2 m/s impact velocity.**

Figure 14 compares pelvis accelerations from the cadaver tests to tests with the THOR-NT and Hybrid III. Figure 15 compares femur accelerations from the tests with cadavers and the two ATDs. The magnitudes of the femur and pelvis accelerations measured from both ATDs are similar to those measured in similar cadaver tests. However, peak ATD femur and pelvis accelerations occur later than peak cadaver femur and pelvis accelerations. In addition, both the THOR and Hybrid III femur and pelvis accelerations peak at the same time applied force peaks, while applied force peaks after femur and pelvis accelerations in all cadaver tests.





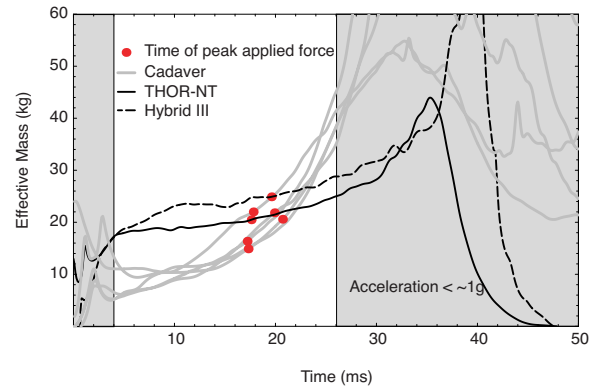
**Figure 14. Comparison of cadaver pelvis accelerations with pelvis accelerations histories from THOR-NT and Hybrid III at the 1.2 m/s impact velocity.**



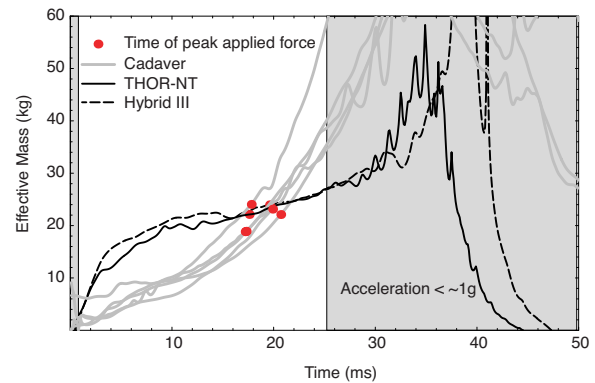
**Figure 15. Comparison of cadaver femur accelerations with femur accelerations histories from THOR-NT and Hybrid III at the 1.2 m/s impact velocity.**

Figure 16 compares the effective mass histories calculated using the pelvis accelerations from the THOR, Hybrid III and cadavers, while Figure 17 compares the effective mass histories calculated using femur acceleration. Effective mass calculated using femur and pelvis accelerations from ATDs increases rapidly during the early part of the effective mass history and then gradually increased for the remainder of impact loading.

Table 4 compares the Hybrid III and THOR effective masses at the time of peak applied force calculated using femur and pelvis accelerations. The Hybrid III effective masses at the time of peak force calculated using pelvis and femur accelerations are 24.9 kg (Range: 24.6-25.3 kg) and 24.0 kg (Range: 23.5-24.5 kg), respectively. The THOR effective masses at the time of peak force calculated using pelvis and femur accelerations are 20.5 kg (Range: 20.1-21.2 kg) and 22.0 kg (Range: 21.7-22.7 kg), respectively. These values are similar to the overall average cadaver effective mass calculated using similar methods.



**Figure 16. Pelvis-acceleration-based effective-mass histories from THOR-NT and Hybrid III compared to cadaver effective mass histories at the 1.2 m/s impact velocity.**



**Figure 17. Femur-acceleration-based effective-mass histories from THOR-NT and Hybrid III compared to cadaver effective mass histories at the 1.2 m/s impact velocity.**

**Table 4. Effective Mass From Cadaver and ATD Tests at the Time of Peak Force at the 1.2 m/s Impact Velocity**

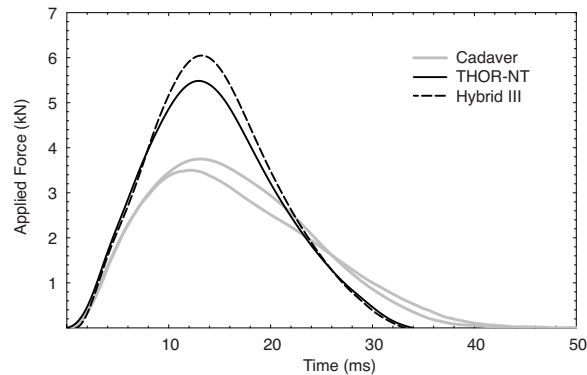
Subject	Calculated with Pelvis Acceleration kg (Min-Max)	Calculated with Femur Acceleration, kg (Min-Max)
Overall Average Cadaver	20.4 (17.2-26.1)	21.4 (14.9-23.3)
Hybrid III	24.9 (25.3-24.6)	24.0 (23.5-24.5)
THOR-NT	20.5 (20.1-21.2)	22.1 (21.7-22.7)

### 3.5 m/s Knee Impacts

Figure 18 compares the applied force histories from the THOR-NT and Hybrid III to the applied force histories from the cadavers for tests at the 3.5 m/s knee impact velocity. Peak applied forces produced by impacts to the THOR and Hybrid III knees were 5.5 kN, and 6.1 kN, respectively. In comparison,



peak forces produced in the cadaver tests were 3.5 and 3.8 kN.



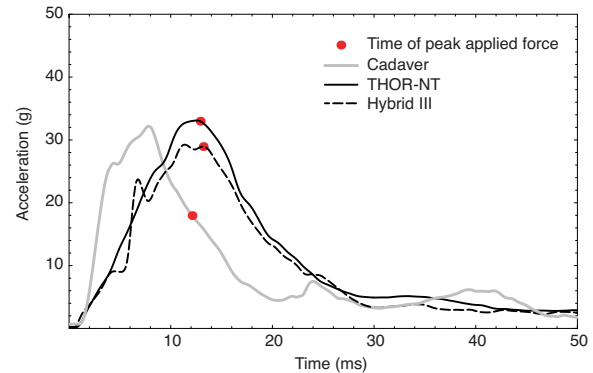
**Figure 18. Comparison of applied force histories from cadaver, THOR-NT and Hybrid III at the 3.5 m/s impact velocity.**

Figure 19 compares pelvis accelerations from the Hybrid III and THOR-NT with pelvis acceleration from the single cadaver that produced usable pelvis acceleration data at the 3.5 m/s knee impact velocity. Figure 20 compares the femur accelerations from the THOR and Hybrid III with similar quantities from the cadaver tests. Similar to the 1.2 m/s responses, the peak ATD femur and pelvis accelerations are similar in magnitude to the peak cadaver femur and pelvis accelerations. Also like the 1.2 m/s knee impacts, the peak ATD femur and pelvis accelerations occur at the same times as peak applied force while the peak cadaver femur and pelvis accelerations occur approximately 6 ms earlier in the impact event than peak applied force.

Figures 21 and 22 compare effective mass histories from cadavers and ATDs calculated using pelvis and femur accelerations, respectively. Similar to the results from 1.2 m/s testing, effective mass calculated using femur and pelvis accelerations from ATDs increased rapidly during the early part of the effective mass history followed by a gradual increase in effective mass until after the time of peak force. Table 5 lists ATD and cadaver effective masses at the time of peak force calculated using femur and pelvis accelerations from the 3.5 m/s tests. The effective masses at the time of peak force calculated using Hybrid III and THOR pelvis accelerations are 23.0 kg (Range: 20.1-20.5 kg) and 17.0 kg (Range: 16.4-17.4 kg). These values and the ranges of these values are similar to the effective mass from Subject 4 calculated under similar loading conditions.

The effective masses at the time of peak force calculated using Hybrid III and THOR femur

accelerations are 21.3 (Range 20.7-21.8) and 17.0 kg 19.0 (Range 18.4-19.2). These values and the ranges of these values are similar to the effective mass from Subjects 4 and 5 calculated under similar loading conditions.



**Figure 19. Comparison of cadaver pelvis accelerations with pelvis accelerations histories from THOR-NT and Hybrid III at the 3.5 m/s impact velocity.**

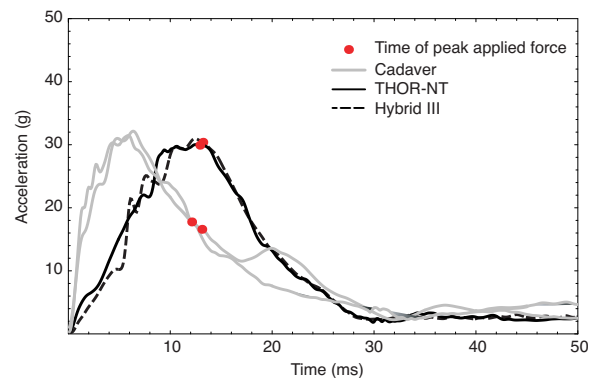


**Figure 20. Comparison of cadaver femur accelerations with femur accelerations histories from THOR-NT and Hybrid III at the 3.5 m/s impact velocity.**

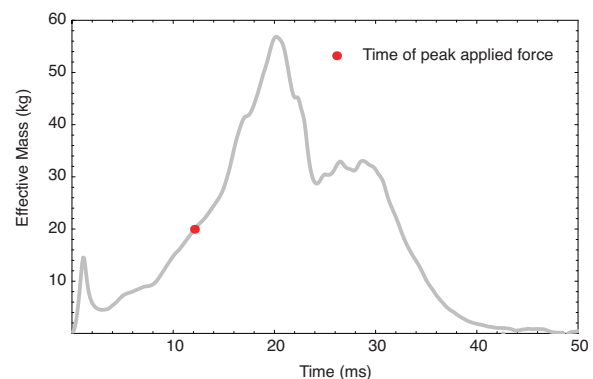


**Figure 21. Pelvis-acceleration-based effective-mass histories from THOR-NT and Hybrid III compared to cadaver effective mass histories at the 3.5 m/s impact velocity.**

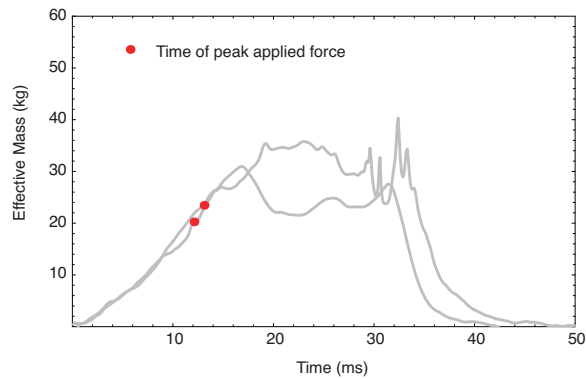


**Figure 22. Femur-acceleration-based effective-mass histories from THOR-NT and Hybrid III compared to cadaver effective mass histories at the 3.5 m/s impact velocity.**

**Table 5. Effective Mass From Cadaver and ATD Tests at the Time of Peak Force at the 3.5 m/s Impact Velocity**

Subject	Calculated with Pelvis Acceleration, kg (Max-Min)	Calculated with Femur Acceleration, kg (Max-Min)
4		23.5 (22.5-24.4)
5	20.0 (19.2-21.3)	20.3 (19.8-22.2)
Hybrid III	20.3 (20.1-20.5)	21.3 (20.7-21.8)
THOR-NT	17.0 (16.7-17.4)	19.0 (18.4-19.2)

## DISCUSSION

The inertial responses of five midsize male cadavers and the Hybrid III and THOR-NT midsize male ATDs were characterized and compared using symmetric knee impacts with 275-kg flat-faced-padded impactor at velocities of 1.2 m/s and 3.5 m/s. The combination of impactor velocity and the padding on the knee impact surfaces in the 1.2 m/s tests were selected to ensure that no KTH injuries would be produced. However, this loading condition was associated with Hybrid III peak femur load cell forces and loading rates of 1.3 kN and 85 N/ms, which are substantially lower than the 3-6 kN range of peak forces and the 200-600 N/ms range of loading rates in FMVSS 208 and NCAP tests. Because these less severe 1.2 m/s impacts produced a different inertial response, two of the five cadavers used in this study were also tested at a 3.5 m/s knee impact velocity, which resulted in peak Hybrid III femur forces and loading rates of 5 kN and 500 N/ms, which are in the range of femur forces and loading rates that are typically found in FMVSS 208 and NCAP tests.

Because none of the knee impacts resulted in knee, thigh, or hip fractures, it was possible to repeatedly impact each cadaver to obtain a set of three to five knee impacts where the phasing of the forces applied to the left and right knees was similar. Data from each pair of symmetric left and right knee impacts on the same cadaver were similar and were therefore averaged to obtain an single set of applied force, femur and pelvis accelerations, and effective mass histories calculated using the applied force and femur and pelvis accelerations.

All of the cadavers used in this study were midsize United States males in stature and within 12 kg of midsize United States male mass. Because the inertial response of the cadavers to knee impact is expected to vary substantially with subject mass, an effort was made to normalize subject response data using equal-stress equal velocity techniques. However, this normalization increased the scatter in the 1.2 m/s response data and was therefore not used to scale either the 1.2 m/s or 3.5 m/s cadaver responses.

For the 1.2 m/s tests, cadavers produced peak forces of approximately 940 N while the THOR-NT and Hybrid III produced peak knee impact forces of approximately 1.4 kN and 1.6 kN, respectively. Peak femur and peak pelvis accelerations for all cadavers and the ATDs were between 6 and 8 g. In the two cadaver tests at the 3.5 m/s impact velocity, the cadaver peak knee impact forces were 3.5 and 3.8 kN. In comparison, the peak forces produced in the 3.5 m/s impacts to the THOR and Hybrid III knees were 5.5 and 6.1 kN, respectively. Peak femur and pelvis accelerations for the cadaver and both ATDs were between 29 g and 32 g.

In both the 1.2 and the 3.5 m/s impacts, peak force applied to the cadaver knees occurred after peak femur and pelvis acceleration while in the ATDs, peak force and peak accelerations occurred at the same time. The similarity in the timing of peak applied forces and accelerations in the ATDs indicates that most of the mass in the ATDs is tightly coupled to the skeletal knee-thigh-hip. The difference in timing between femur and pelvis accelerations and applied force in the cadaver is likely because there is mass in the cadaver that is initially loosely coupled to the skeleton and that becomes more tightly coupled to the skeleton as it moves.

The shapes of the cadaver effective mass histories were similar for both the 1.2 m/s and 3.5 m/s tests.

Early in the impact event, effective mass calculated using both cadaver pelvis and femur acceleration was low and then increased until after the time of peak force. Because cadaver femur acceleration leads pelvis acceleration by approximately 2 ms during the loading portion of all tests, the low initial effective mass is due to coupling of the femur to the impactor. The subsequent increase in effective mass is likely from coupling of the pelvis to the displacing femur. In addition, coupling of flesh mass to the thigh and pelvis, coupling of torso mass to the pelvis, and coupling of the leg to the knee likely account for some of the increase in effective mass that occurs following the initial portion of the effective mass history.

ATD effective mass histories at both impact velocities are different than cadaver effective mass histories. During the early part of the knee impact event, ATD effective mass is much higher than cadaver effective mass. As the impact event progresses, ATD effective mass gradually increases until, at the time of peak force, ATD and cadaver effective masses are within approximately 20% of each other.

The initial rapid increase in ATD effective mass is because most mass in the ATD KTH is rigidly coupled to the skeletal femur and pelvis, which under knee impact, immediately couple to the impactor. High-speed video suggests that the subsequent gradual increase in ATD effective mass is from the leg and torso coupling to the skeletal femur and pelvis, respectively.

Comparisons of effective mass histories from tests at 1.2 m/s and 3.5 m/s performed on the same two subjects indicate that more severe knee loading conditions result in larger effective mass values at the time of peak force. This likely occurs because more severe knee loading conditions result in higher skeletal KTH displacements at the time of peak force, which likely couple additional mass to the KTH. The differences in KTH effective mass response with knee impact severity suggest that comparisons between ATD and cadaver knee impact response should be made using loading conditions that are representative of the knee loading conditions that occur in the real world, such as the 3.5 m/s knee impacts. To make comparisons between the cadaver and ATDs, it is necessary to develop corridors that characterize the variability of cadaver responses. However, because only two subjects were tested at the 3.5 m/s impact velocity, more data are needed before corridors can be developed.

Comparisons between ATD and cadaver responses suggest that ATDs can be made to respond more like cadavers by decreasing the mass that is tightly coupled to the femur and pelvis. However, the knee/femur stiffness of the Hybrid III is 8-12 times greater than the knee stiffness of the cadaver and the knee/femur stiffness of the THOR- $\alpha$ /THOR-NT is 2-3 times greater (Rupp et al. 2003b) than that of the cadaver. Therefore, decreasing the coupling between skeletal and flesh mass in ATD may not alone be sufficient to make ATD knee impact forces similar to cadaver knee impact forces.

The effective mass response of the cadaver may be substantially different from the effective mass response of a living human because of muscle tension, which would tend to increase the coupling of the thigh and pelvis flesh to the skeletal KTH. It may therefore be advisable to develop computational models of the lower extremities that can simulate the effect of muscle tension on response of the KTH to knee impact loading. These models could then be used to suggest how to redesign ATDs to better mimic living humans rather than cadavers.

Although cadaver femur force was not measured in this study, the peak cadaver femur force at the 3.5 m/s impact velocity will be less than the peak cadaver applied force of 3.5 kN to 3.8 kN. Because peak femur load cell forces measured by the Hybrid III and THOR under similar loading conditions were substantially greater than 3.8 kN, it can be inferred that ATDs and cadavers produce different forces at the femur load cell location. Therefore, either femur force measurements from the Hybrid III and THOR-NT will need to be scaled to be used with force-based injury criteria developed from cadaver tests or the Hybrid III and THOR will need to be modified to respond more like a living human.

The cadaver data collected in this study can be used to develop models that predict the distribution of forces at any location along the knee-thigh-hip complex for knee impacts that are representative of real-world knee-to-knee bolster impacts. Such models can be also be used with the hip injury tolerance data measured by Rupp et al. (2003a) to predict the risk of hip fracture for knee loading by a knee-bolster-like surface. These models can also be used to optimize knee bolster design to reduce the risk of disabling hip injuries in frontal crashes.

## CONCLUSIONS

The inertial responses of five midsize male cadavers, the Hybrid III midsize male, and the THOR-NT were

characterized and compared using symmetric padded knee impacts at a 1.2 m/s impact velocity. Two of these five cadavers were also impacted at a 3.5 m/s impact velocity using a similar impactor. Using applied force and femur and pelvis acceleration data from these impacts, the following observations and conclusions can be made:

- Knee impact forces produced by the cadaver were substantially less than those produced by the THOR and Hybrid III.
- Femur and pelvis accelerations produced by both dummies and the cadavers were similar in magnitude, but different in phasing. The peak cadaver femur and pelvis accelerations occurred substantially earlier than the time of peak force, while the peak ATD femur and pelvis accelerations occurred at the time of peak force. This behavior suggests that there is loosely coupled mass in the cadaver, but not in either ATD.

## ACKNOWLEDGEMENTS

This research was supported by the National Highway Traffic Safety Administration under contract number DTNH22-99-H-1700.

The authors are grateful to Thomas Jeffreys for his assistance in cadaver preparation and testing. The authors would also like to acknowledge the contributions of Charles Bradley, Brian Eby, Stewart Simonett, and James Whitley who assisted in the data collection and test preparation. The assistance of Kathy Klinich in the review of this manuscript is gratefully acknowledged.

## REFERENCES

- Burgess, A.R., Dischenger P.C., O'Quinn, T.D., and Schmidhauser, C.B. (1995). Lower extremity injuries in drivers of airbag-equipped automobiles: clinical and crash reconstruction correlations. *Journal of Trauma* 38(4): pp 509-516.
- Eppinger, R.H. (1978). Prediction of thoracic injury using measurable parameters. *Proceedings of the 6<sup>th</sup> International Technical Conference on Experimental Safety Vehicles*, pp. 770-780. National Highway Traffic Safety Association, Washington D.C.
- Horsch, J.D. and Partick, L.M. (1976). Cadaver and dummy knee impact response. SAE Paper No. 760799. Society of Automotive Engineers, Warrendale, PA.
- Kuppa, S., Wang, J., Haffner, M., and Eppinger, R. (2001). Lower extremity injuries and associated injury criteria. *Proceedings of the 17<sup>th</sup> International Technical Conference on the Enhanced Safety of Vehicles*, Paper No. 457. National Highway Traffic Safety Administration, Washington, D.C.
- Kuppa, S. and Fessahaie, O. (2003). An overview of knee-thigh-hip injuries in frontal crashes in the United States. *Proceedings of the 18<sup>th</sup> International Technical Conference on Experimental Safety Vehicles*. National Highway Traffic Safety Association, Washington D.C.
- Read, K. M., Burgess, A. R., Dischinger, P. C., Kufera, J. A., Kerns, T. J., Ho, S. M., and Burch, C. (2002). Psychosocial and physical factors associated with lower extremity injury. *Proceedings of the 46<sup>th</sup> Annual Conference of the Association for the Advancement of Automotive Medicine*, pp. 289-303. Association for the Advancement of Automotive Medicine. Des Plaines, IL
- Rupp, J.D., Reed, M.P., Van Ee, C.A., Kuppa, S., Wang, S.C., Goulet, J.A., and Schneider, L.W. (2002). The tolerance of the human hip to dynamic knee loading. *Stapp Car Crash Journal* 46, 211-228.
- Rupp, J.D. Reed M.P., Jeffreys T.J., and Schneider L.W (2003a). Effects of Hip Posture on the Frontal Impact Tolerance of the Human Hip Joint. *Stapp Car Crash Journal* 47. pp 21-33.
- Rupp, J.D., Reed, M.P., Madura, N.H., Kuppa, S., and Schneider L.W. (2003b) Comparison of knee/femur force-deflection response of the Thor, Hybrid III, and human cadaver to dynamic frontal-impact knee loading. *Proceedings of the 18th International Conference of Experimental Safety Vehicles*. National Highway Traffic Safety Administration, Washington DC.
- Shams, T. (2004) Personal communication on force-deflection response of the THOR-NT femur puck.
- Society of Automotive Engineers Dummy Testing Equipment Subcommittee (1998). User's manual for the midsize Hybrid III test dummy, Engineering Aid 23. Society of Automotive Engineers, Warrendale, PA.

## APPENDIX

The following plots illustrate the variation in cadaver applied force, femur and pelvis acceleration, and effective mass responses from a single subject.

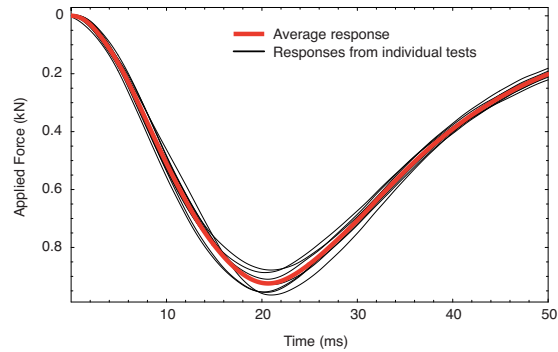


**Figure A1.** Left and Right knee impact forces from all tests performed on Subject 3 relative to the associated average knee impact force.

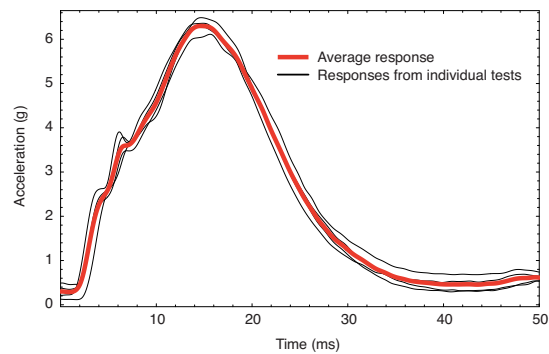


**Figure A2.** Pelvis accelerations from all tests performed on Subject 3 relative to the associated average pelvis acceleration.

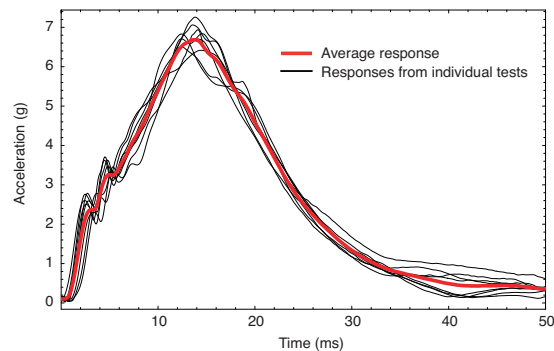


**Figure A3.** Left and Right femur accelerations from all tests performed on Subject 3 relative to the associated average femur acceleration.

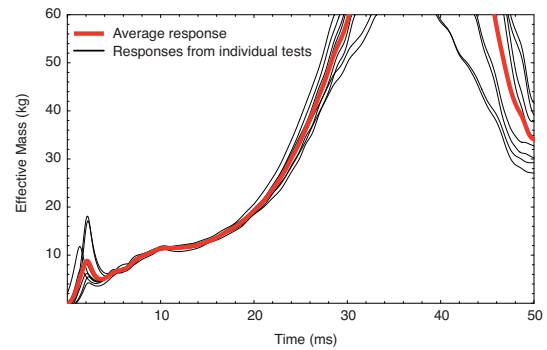


**Figure A4.** Left and Right pelvis-acceleration-based effective-mass histories from all tests performed on Subject 3 relative to the associated average pelvis-acceleration-based effective-mass history.

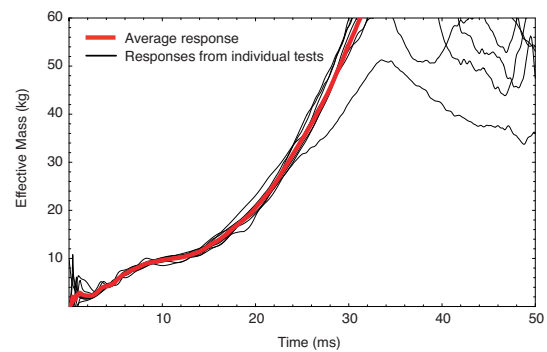


**Figure A5.** Left and Right femur-acceleration-based effective-mass histories from all tests performed on Subject 3 relative to the associated average femur-acceleration-based effective-mass history.

